Molecular Cell, Volume *71*

Supplemental Information

In Vivo Evidence for ATPase-Dependent DNA Translocation by the *Bacillus subtilis* SMC Condensin Complex

Xindan Wang, Anna C. Hughes, Hugo B. Brandão, Benjamin Walker, Carrie Lierz, Jared C. Cochran, Martha G. Oakley, Andrew C. Kruse, and David Z. Rudner

Figure S1

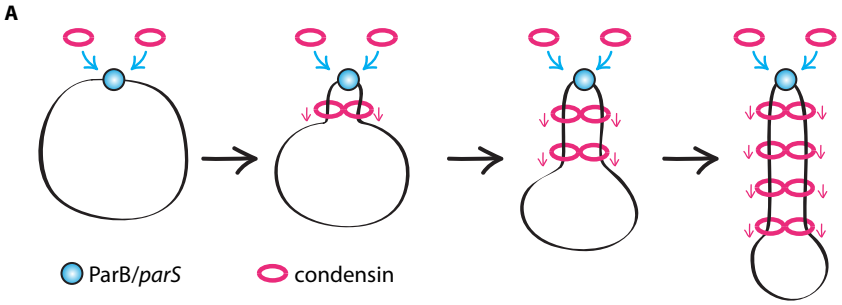

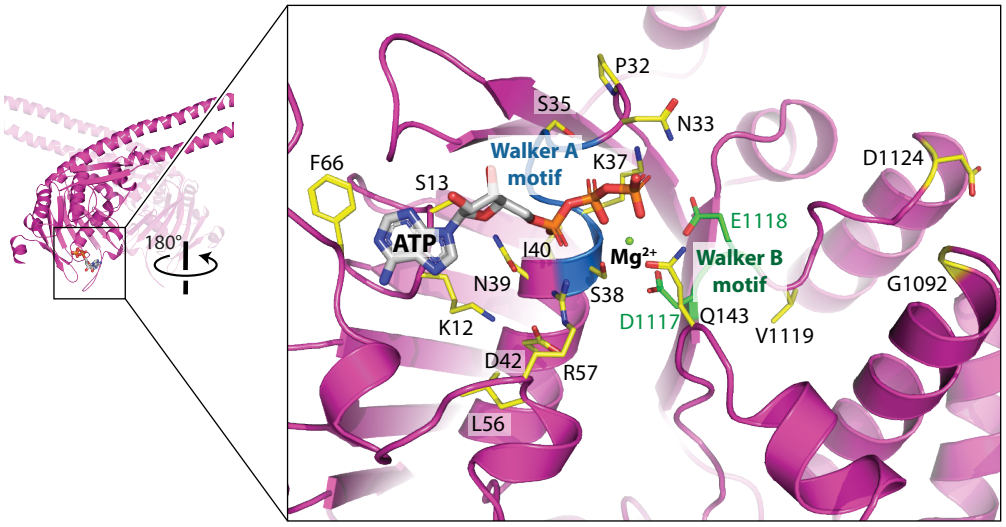

C

Mutant	Phenotype
SMC (N33A)	very slow growth in ParB⁺ background; similar to *Δsmc*
SMC (K37A)	
SMC (K37I)	
SMC (S38A)	
SMC (N39A)	
SMC (G1092S)	
SMC (D1124E)	
SMC (P32A)	slow growth in ParB⁺ background; no growth in ParB⁻
SMC (P32G)	
SMC (Q143A)	
SMC (V1119L)	
SMC (K12R)	similar to WT in ParB⁺ background; slow growth upon ParB depletion
SMC (R57A)	
SMC (R57K)	
SMC (D42A)	
SMC (F66Y)	similar to WT in ParB⁺ background; mild growth defect upon ParB depletion
SMC (S13A)	similar to WT in the presence and absence of ParB
SMC (S35A)	
SMC (I40V)	
SMC (D42E)	
SMC (L56V)	

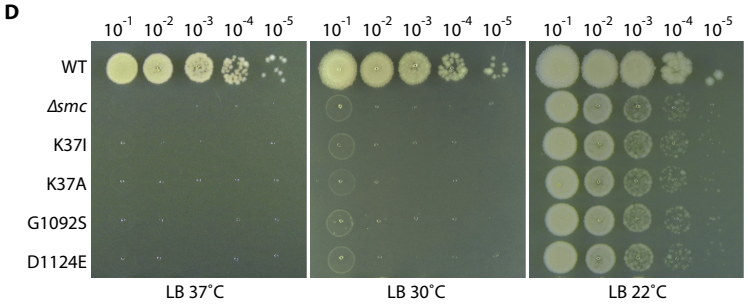

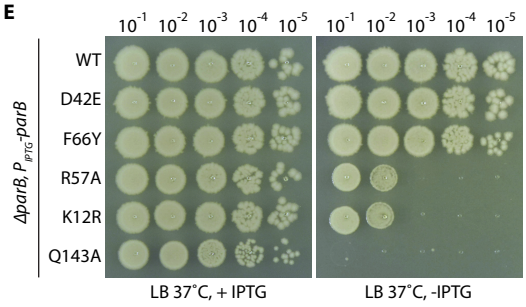

Figure S1. Rational design and characterization of SMC ATPase mutants. Related to Figure 1. A, Schematic model of condensin-dependent loop formation in *B. subtilis*. Condensin is loaded onto the chromosomes by ParB bound to the centromeric *parS* site. Once loaded, the complex travels down the left and right chromosome arms while tethering them together. Double rings are depicted in the model but the architecture of the loop-forming complex is not known. **B,** Homology model of the ATPase domain of *B. subtilis* SMC generated using the apo-structure of *B. subtilis* SMC (PDB ID 3ZGX) (Burmann et al., 2013) and *Pyrococcus furiosus* SMC in complex with ATP (PDB ID 1XEX) (Lammens et al., 2004). A bound ATP and Mg^{2+} ion were included during modeling as rigid bodies, positioned based on the *P. furiosus* SMC structure. Walker A and B motifs are highlighted in blue and green, respectively. Amino acids highlighted in yellow were individually mutated and tested. **C,** Table of growth phenotypes associated with the mutants in a strain harboring an IPTG-inducible *parB* gene. Cells were grown in the presence or absence of inducer on LB agar plates at 37˚C. Mutants with similar phenotypes are grouped together from most severe (dark grey) to indistinguishable from wild-type (white). **D,** Spot dilutions of representative SMC mutants. Strains containing wild-type or indicated SMC mutants were grown in LB medium at 22˚C. Cultures were normalized to an OD_{600} of 2, then serial diluted and spotted on LB plates, and incubated at 37˚C, 30˚C or 22˚C. The catalytic mutants K37I and K37A, the signature motif mutant G1092S, and the D-loop mutant D1124E had phenotypes similar to the Δ*smc* mutant. **E,** Spot dilutions of indicated SMC mutants. Strains containing wild-type or indicated SMC mutants, and harboring an IPTG-inducible *parB* gene were grown in LB medium at 37˚C in the presence of 1 mM IPTG. Cells were washed 3 times in LB, normalized to an OD_{600} of 2, and serially diluted. 5 µl of each dilution was spotted on LB agar plates with or without 1 mM IPTG. The plates were incubated at 37˚C for 12 h.

Figure S2

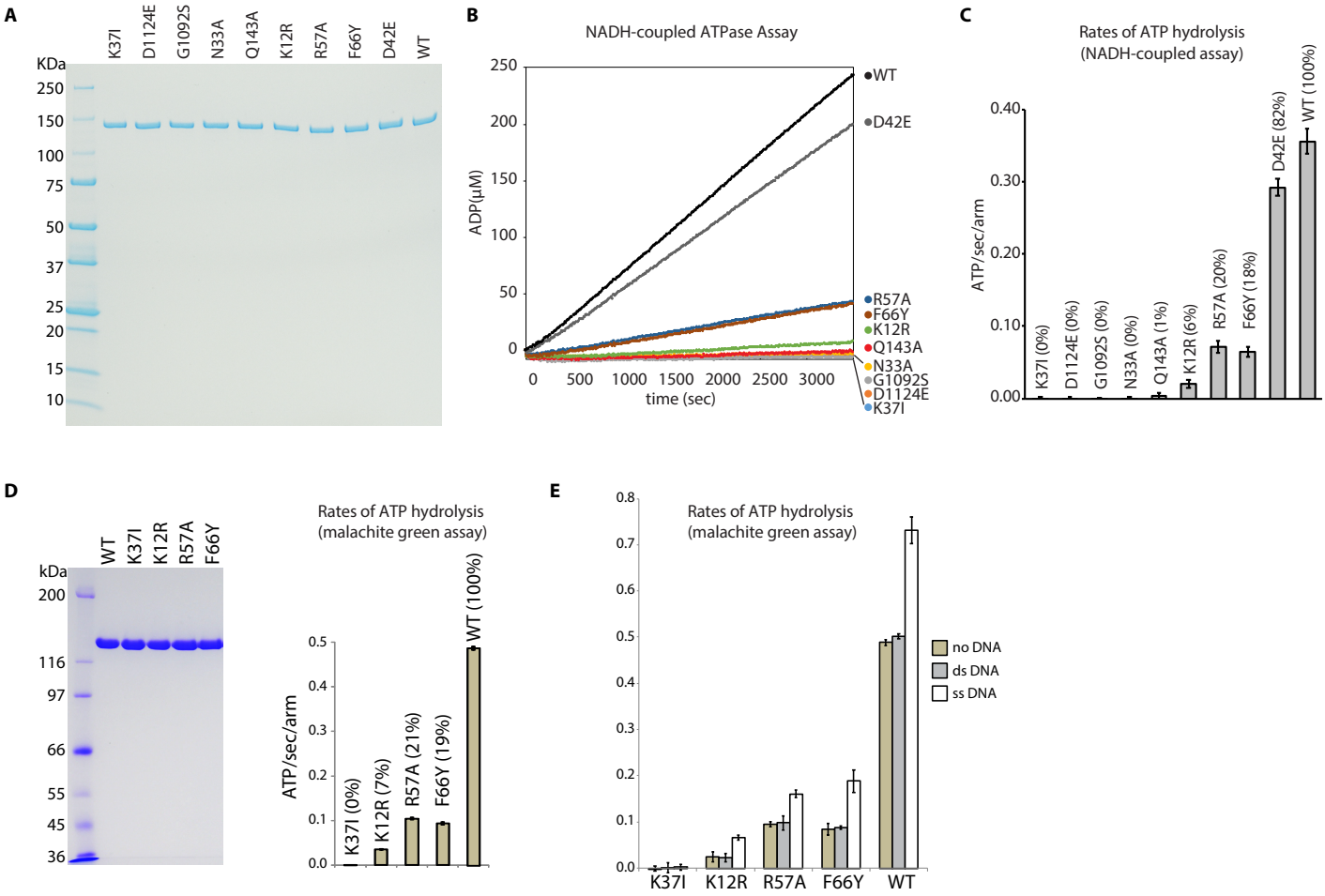
A
K37I
D1124E
G1092S
N33A
Q143A
K12R
R57A
F66Y
D42E
WT
KDa
250
150
100
75
50
37
25
20
15
10
B
NADH-coupled ATPase Assay
ADP(μM)
time (sec)
WT
D42E
R57A
F66Y
K12R
Q143A
N33A
G1092S
D1124E
K37I
C
Rates of ATP hydrolysis
(NADH-coupled assay)
ATP/sec/arm
K37I (0%)
D1124E (0%)
G1092S (0%)
N33A (0%)
Q143A (1%)
K12R (6%)
R57A (20%)
F66Y (18%)
D42E (82%)
WT (100%)
D
WT
K37I
K12R
R57A
F66Y
kDa
200
116
97
66
55
45
36
Rates of ATP hydrolysis
(malachite green assay)
ATP/sec/arm
K37I (0%)
K12R (7%)
R57A (21%)
F66Y (19%)
WT (100%)
E
Rates of ATP hydrolysis
(malachite green assay)
no DNA
ds DNA
ss DNA
K37I
K12R
R57A
F66Y
WT

Figure S2. ATPase rates of SMC mutants. Related to Figure 1.

A, Protein gel of recombinant SMC-His_6 and point mutants. 0.5 µg of purified proteins were loaded onto 4-20% Tris-glycine gradient gel, stained with InstantBlue Protein Stain (Expedeon). **B,** NADH-coupled ATPase assays (see Methods). ADP product formed was plotted against time (second). The graph represents the average of two technical replicates from one experiment. **C,** Bar graph showing ATPase rates calculated using NADH-coupled ATPase assay in **B**. Error bars show the standard deviation of four independent experiments using frozen aliquots of proteins from the same protein preparations. Numbers in brackets indicate the ATPase rates of the mutants relative to the wild-type. **D,** ATPase rates measured using malachite green assay. Coomassie-stained gel of wild-type SMC and indicated mutants from a separate purification. The ATPase rates of the purified proteins were measured using malachite green assay (see Methods). Numbers in brackets indicate the ATPase rates of the mutants relative to the wild-type. Error bars show the standard deviation of three replicates. **E,** ATPase rates in the presence or absence of DNA. Proteins in **D** were used to perform malachite green ATPase assay in the presence or absence of 15.6 µM of double-stranded DNA (dsDNA; ΦX174 RF I DNA; NEB N3021L) or single-stranded DNA (ssDNA; ΦX174 viron DNA; NEB N3023L).

Figure S3

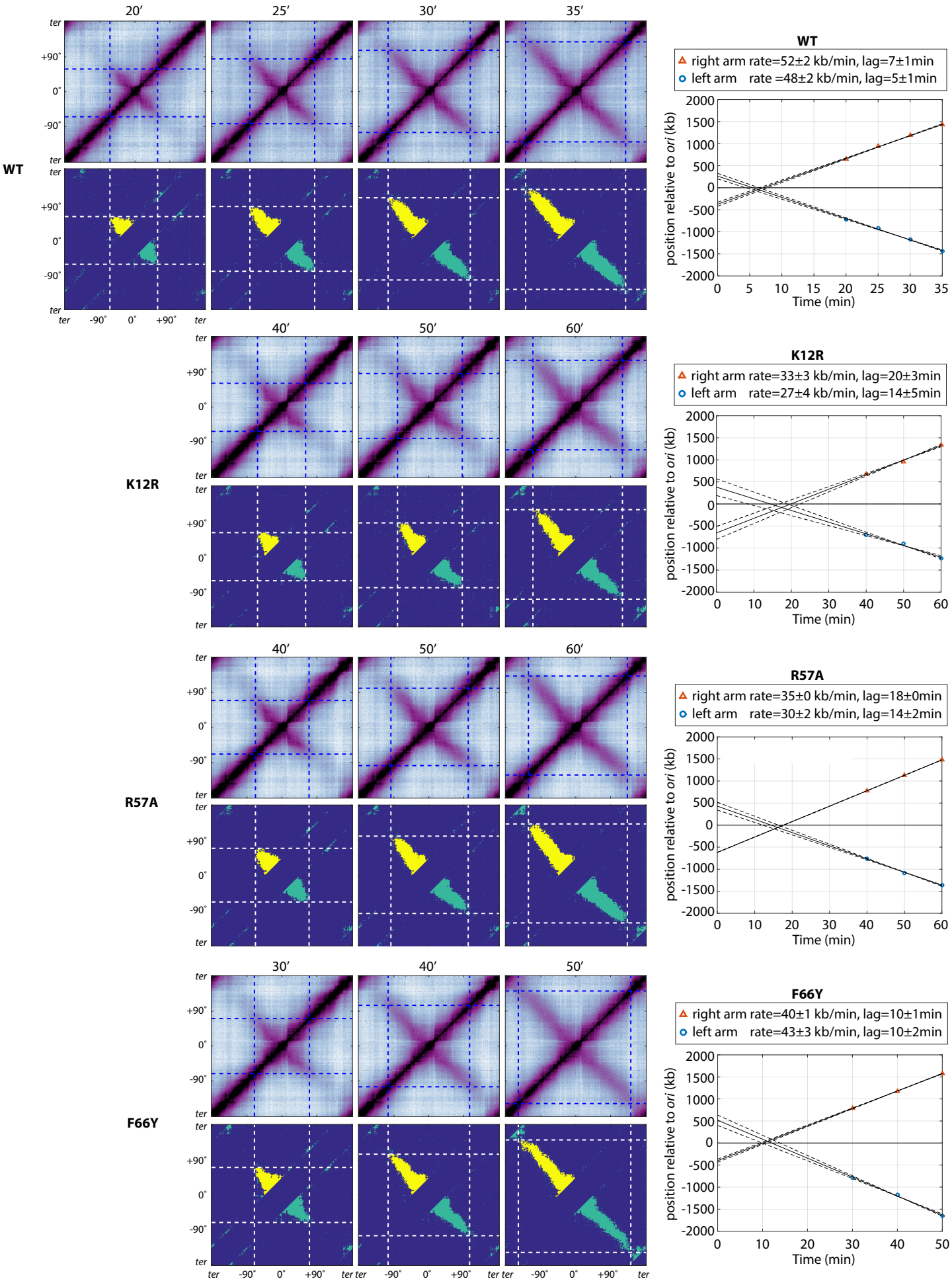
WT
20′
25′
30′
35′
ter
+90°
0°
-90°
ter -90° 0° +90° ter
WT
right arm rate=52±2 kb/min, lag=7±1min
left arm rate =48±2 kb/min, lag=5±1min
position relative to ori (kb)
Time (min)
K12R
40′
50′
60′
K12R
right arm rate=33±3 kb/min, lag=20±3min
left arm rate=27±4 kb/min, lag=14±5min
R57A
40′
50′
60′
R57A
right arm rate=35±0 kb/min, lag=18±0min
left arm rate=30±2 kb/min, lag=14±2min
F66Y
30′
40′
50′
F66Y
right arm rate=40±1 kb/min, lag=10±1min
left arm rate=43±3 kb/min, lag=10±2min

Figure S3. Analysis of the rate of DNA juxtaposition. Related to Figure 2.

The endpoints of DNA juxtaposition after ParB induction (from Figure 2A, B) were determined as described in the Methods, using a threshold of 0.5x standard deviation (σ) above the mean Hi-C score. Lower panels are binary maps showing points (light green and yellow) with Hi-C interactions scores above the specified threshold. Neighboring points that were separated by less than 5 pixels were connected. The largest region of inter-connected points (highlighted in yellow) was identified as the Hi-C enrichment region due to DNA juxtaposition. The enrichment endpoints are indicated with white dotted lines. For visualization, these positions were marked with blue dotted lines on the Hi-C contact maps in the upper panels. The positions (relative to the replication origin) were plotted on the graphs to the right. An endpoint position on the right arm is labeled as a positive value, and on the left arm as a negative value. The rates and errors for the DNA juxtaposition were calculated from the slope of the line-of-best-fit and the standard error of the regression, respectively. The leading edges of the DNA juxtaposition in the SMC mutants were less well defined than wild-type in this study and our previous study (Wang et al., 2017). We suspect that this is due to greater heterogeneity in loading and translocation. Accordingly, a less stringent threshold of 0.5xσ was used in this analysis.

Figure S4

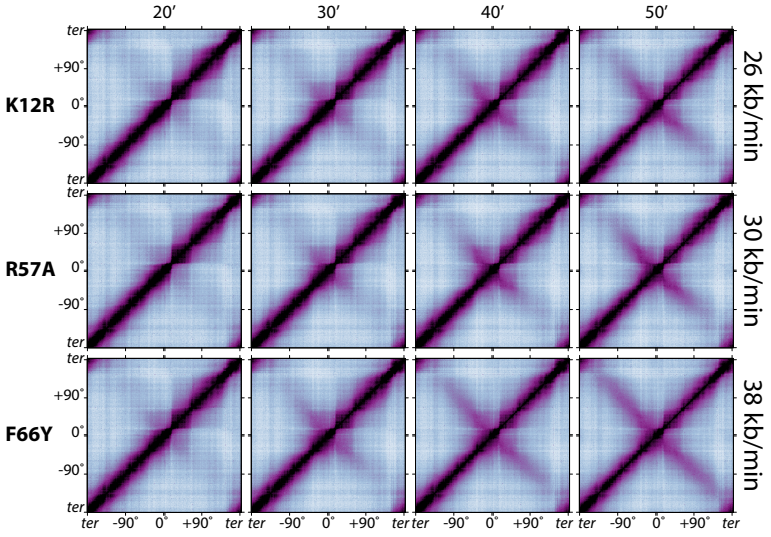

Figure S4. Rate of DNA juxtaposition is reproducible. Related to Figure 2. Hi-C contact maps from an independent experiment are shown. The rates of DNA juxtaposition are indicated on the right.

Figure S5

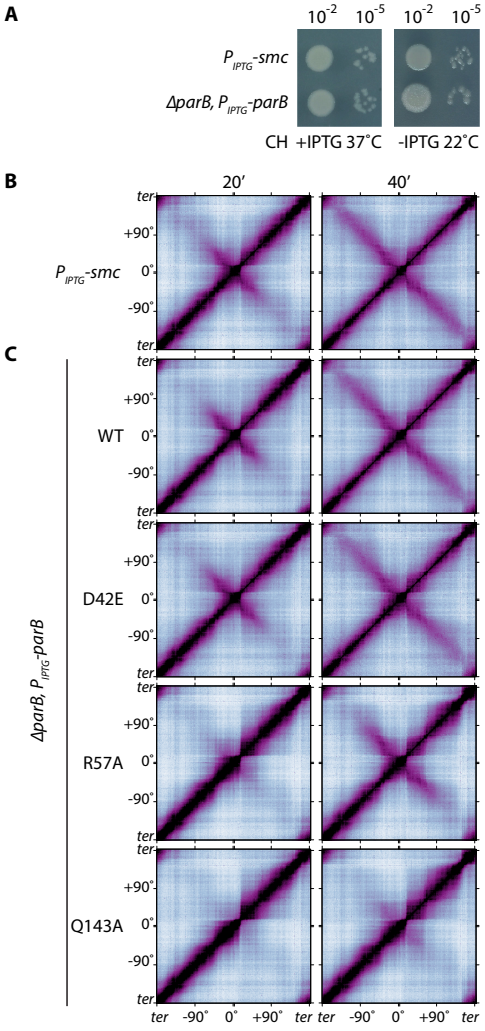
A
10-2
10-5
10-2
10-5
PIPTG-smc
ΔparB, PIPTG-parB
CH +IPTG 37°C
-IPTG 22°C
B
20′
40′
PIPTG-smc
C
ΔparB, PIPTG-parB
WT
D42E
R57A
Q143A
ter
+90°
0°
-90°

Figure S5. Controls for Hi-C experiments. Related to Figure 2.

A, Spot dilutions of the indicated strains on CH agar plates. The 10^{-2} and 10^{-5} dilutions are shown. To test the growth of cells for Hi-C experiments, indicated strains were grown in CH liquid medium at 22˚C, normalized to an OD_{600} of 2 and spotted on CH plates with or without IPTG and incubated at 37˚C and 22˚C respectively. The *smc* depletion strain, which harbors an IPTG inducible *smc* gene grew similarly to *parB* depletion strain, which harbors an IPTG inducible *parB* gene. **B and C,** Hi-C contact maps from the indicated strains. Cells were first grown in liquid CH medium at 22˚C without IPTG. Then IPTG was added to 1 mM final concentration and the cultures were placed at 37˚C. Samples were collected for Hi-C at 20 min and 40 min after IPTG addition. **B,** Hi-C contact map of the *smc* depletion strain, which contains an IPTG-inducible *smc* gene as the sole source of SMC in an otherwise wild-type background. **C,** Hi-C experiments of *parB* depletion strains, which contain an IPTG-inducible *parB* gene and the indicated SMC mutants.

Table S1. Strains used in this study. Related to Figures 1 and 2.

strain	genotype	reference	figure
BWX4077	*parSΔ9 no a.b., Δspo0J (remains wt parS at -1˚)::spec, yvbJ::Pspank (optRBS) spo0J (ΔparS) cat, smc (WT) loxP-kan-loxP*	this study	1B, 2
BWX4078	*parSΔ9 no a.b., Δspo0J (remains wt parS at -1˚)::spec, yvbJ::Pspank (optRBS) spo0J (ΔparS) cat, smc (R57A) loxP-kan-loxP*	this study	1B, 2
BWX4149	*parSΔ9 no a.b., Δspo0J (remains wt parS at -1˚)::spec, yvbJ::Pspank (optRBS) spo0J (ΔparS) cat, smc (K12R) loxP-kan-loxP*	this study	1B, 2
BWX4152	*parSΔ9 no a.b., Δspo0J (remains wt parS at -1˚)::spec, yvbJ::Pspank (optRBS) spo0J (ΔparS) cat, smc (F66Y) loxP-kan-loxP*	this study	1B, 2
PY79	*wild-type*	(Youngman et al., 1983)	
AG1468	*Δspo0J (remains wt parS at -1˚)::spec, trpC2, pheA1*	(Ireton et al., 1994)	
BWX3976	*smc (WT) loxP-kan-loxP*	this study	
BWX3990	*smc (R57A) loxP-kan-loxP*	this study	
BWX4129	*smc (K12R) loxP-kan-loxP*	this study	
BWX4137	*smc (F66Y) loxP-kan-loxP*	this study	
BWX4070	*parSΔ9 no a.b., Δspo0J (remains wt parS at -1˚)::spec, yvbJ::Pspank (optRBS) spo0J (ΔparS) cat*	this study	

Table S2. Plasmids used in this study. Related to Figures 1 and 2.

plasmid	description	reference
pKM309	*smc-(his)6 (kan)*	(Sullivan et al., 2009)
pWX599	*pelB::Psoj mcherry-spo0J (ΔparS) (cat)*	(Wang et al., 2015)
pWX722	*yvbJ::Pspank (optRBS) spo0J (ΔparS) (cat)*	this study
pWX740	*smc(K12R)-(his)6 (kan)*	this study
pWX741	*smc(R57A)-(his)6 (kan)*	this study
pWX742	*smc(F66Y)-(his)6 (kan)*	this study
pWX743	*smc(K37I)-(his)6 (kan)*	this study
pWX758	*smc(N33A)-(his)6 (kan)*	this study
pWX759	*smc(D42E)-(his)6 (kan)*	this study
pWX760	*smc(Q143A)-(his)6 (kan)*	this study
pWX762	*smc(G1092S)-(his)6 (kan)*	this study
pWX763	*smc(D1124E)-(his)6 (kan)*	this study

Table S3. Oligonucleotides used in this study. Related to STAR methods.

oligos	sequence	use
oWX438	gaccagggagcactggtcaac	universal
oWX439	tccttctgctccctcgctcag	universal
oWX523	cattcaggagtcgagattatcgctcag	sequencing
oWX822	cttttaacctctttcctcgttactgaac	BWX3976
oWX848	gaagagctctctgccgtatctgaaaag	sequencing
oWX999	tttGCTAGCcagagtggaggcaagaacgccttaaccc	pWX722
oWX1194	gggaaagtggaagagatcctgagc	sequencing
oWX1195	cttcacaatgaaaatgtcgaagag	sequencing
oWX1196	gcccggcattcatcatttctcggg	sequencing
oWX1620	tgagcaggtgcctgctgcaaagcg	BWX3976
oWX1621	ctgagcgagggagcagaaggattattgtttcgtatggtgtttttgc	BWX3976
oWX1622	gttgaccagtgctccctggtcaatccccctatgactcaggggatttcag	BWX3976
oWX1623	agcgtcctgctctattggcggatg	BWX3976
oWX1624	ttcgatatcataggcagtcagcgc	BWX3976
oWX1625	gatgttgctttttccgcttcctgccggcccgacaactgctgtcac	pWX758
oWX1626	gggccggcaggaagcggaaaaagcaacatc	pWX758
oWX1631	caaaaatgatgtcttccatttttccgcctgcaagagagcgtgccgattgttc	BWX3990
oWX1633	ggcggaaaaatggaagacatcatttttg	BWX3990
oWX1634	gctcaggatctcttccactttccccgcgctgataatagaaaatgcttc	pWX760
oWX1635	gggaaagtggaagagatcctgagc	pWX760
oWX1661	tttgcagaacggatttccgtagac	BWX4129
oWX1666	gccattcgctgggttctcggcgaac	pWX759
oWX1667	ttcgccgagaacccagcgaatggcttccgtgatgttgctttttcc	pWX759
oWX1668	aaaCCCGGGacataaggaggaactactatggctaaaggccttggaaaaggg	pWX722
oWX1696	cgccgtatctgtgctctctcttattggaagtatttctctaatcc	BWX4129
oWX1702	ctttcttgaatcactcccagcataaatgatgtcttccatttttcc	BWX4137
oWX1703	gctgggagtgattcaagaaagcg	BWX4137
oWX1732	ggaaatccgttctgcaaatgatctaaatcctataacgtctaaacg	pWX740
oWX1733	cgtttagacgttataggatttagatcatttgcagaacggatttcc	pWX740
oWX1736	gatgtcttccatttttccgcctgcaagagagcgtgccgattgttc	pWX741
oWX1737	gaacaatcggcacgctctcttgcaggcggaaaaatggaagacatc	pWX741
oWX1738	ctttcttgaatcactcccagcataaatgatgtcttccatttttcc	pWX742
oWX1739	ggaaaaatggaagacatcatttatgctgggagtgattcaagaaag	pWX742
oWX1744	gaatggcatccgtgatgttgctgattccgcttccgttcggcccgac	pWX743
oWX1745	gtcgggccgaacggaagcggaatcagcaacatcacggatgccattc	pWX743
oWX1746	ggcgtagaggatcgagatctcg	sequencing
oWX1747	ccggatatagttcctcctttcagc	sequencing
oWX1792	cgctatagcagtaagcgcacgctctgagcctgacaggaggtttaagttttg	pWX762
oWX1793	gagcgtgcgcttactgctatagcg	pWX762
oWX1794	cgcaaatcggaacacattcgcttcttcgagcgcagcctctacttc	pWX763
oWX1795	gaagtagaggctgcgctcgaagaagcgaatgtgttccgatttgcg	pWX763

Restriction endonuclease sites are capitalized.